BOSTER
antibody and ELISA experts

BOSTER BIOLOGICAL TECHNOLOGY
3942 B Valley Ave, Pleasanton, CA 94566
888-466-3604 | support@bosterbio.com | www.bosterbio.com

Anti-PCNA Antibody (Monoclonal, PC 10)

Catalog Number: MA1083

About Pcna

Proliferating cell nuclear antigen (PCNA) was originally identified by immunofluorescence as a nuclear protein whose appearance correlated with the proliferative state of the cell. PCNA/cyclin has been localized by in situ hybridization to the short arm of human chromosome 20 with a peak of grains over band 20p13. PCNA gene is present in single copy and has 6 exons. It spans 4,961 bp. Synthesis of the nuclear protein cyclin and DNA in quiescent mouse fibroblasts is coordinately induced by serum and purified growth factors. PCNA controls establishment of sister chromatid cohesion during S phase.

Overview

Product Name	Anti-PCNA Antibody (Monoclonal, PC 10)
Reactive Species	Human, Mouse, Rat
Description	Boster Bio Anti-PCNA Antibody (Monoclonal, PC 10) catalog # MA1083. Tested in IHC, ICC, WB applications. This antibody reacts with Human, Mouse, Rat.
Application	IHC, ICC, WB
Clonality	Monoclonal PC 10
Formulation	Mouse IgG in stabilizing components, 1.2% sodium acetate and 0.01mg NaN3.
Storage Instructions	Store at -20˚C for one year from date of receipt. After reconstitution, at 4˚C for one month. It can also be aliquotted and stored frozen at -20˚C for six months. Avoid repeated freeze-thaw cycles.
Host	Mouse
Uniprot ID	P04961

Technical Details

Immunogen	Protein A fusion protein.
Recommended Detection Systems	Boster recommends Enhanced Chemiluminescent Kit with anti-Mouse IgG (EK1001) for Western blot, and HRP Conjugated anti-Mouse IgG Super Vision Assay Kit (SV0001-1) for IHC(P), IHC(F) and ICC.
Cross Reactivity	No cross-reactivity with other proteins
Isotype	Mouse IgG2a
Form	Lyophilized
Concentration	Adding 1 ml of PBS buffer will yield a concentration of 100 ug/ml.
Purification	Ascites

BOSTER BIOLOGICAL TECHNOLOGY
3942 B Valley Ave, Pleasanton, CA 94566
888-466-3604 | support@bosterbio.com | www.bosterbio.com

Suggested Dilutions	Immunohistochemistry (Paraffin-embedded Section), 0.4-1ug/ml, Human, mouse, rat Immunocytochemistry , 1ug/ml, Human, mouse, rat, - Immunohistochemistry (Frozen Section), 0.4-1ug/ml, Human, mouse, rat, - Western blot, 2ug/ml, Human, mouse, rat

BOSTER BIOLOGICAL TECHNOLOGY
3942 B Valley Ave, Pleasanton, CA 94566
888-466-3604 | support@bosterbio.com | www.bosterbio.com

Anti-PCNA Antibody (Monoclonal, PC 10) (MA1083) Images

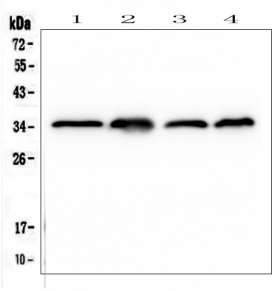

Western blot analysis of PCNA using anti-PCNA antibody (MA1083). Electrophoresis was performed on a 5-20% SDS-PAGE gel at 70V (Stacking gel) / 90V (Resolving gel) for 2-3 hours. The sample well of each lane was loaded with 50ug of sample under reducing conditions. Lane 1: human Caco-2 whole cell lysates, Lane 2: human MDA-MB-231 whole cell lysates, Lane 3: human Jurkat whole cell lysates, Lane 4: human HT1080 whole cell lysates. After Electrophoresis, proteins were transferred to a Nitrocellulose membrane at 150mA for 50-90 minutes. Blocked the membrane with 5% Non-fat Milk/ TBS for 1.5 hour at RT. The membrane was incubated with mouse anti-PCNA antigen affinity purified monoclonal antibody (Catalog # MA1083) at 0.5 ug/mL overnight at 4°C, then washed with TBS-0.1%Tween 3 times with 5 minutes each and probed with a goat anti-mouse IgG-HRP secondary antibody at a dilution of 1:10000 for 1.5 hour at RT. The signal is developed using an Enhanced Chemiluminescent detection (ECL) kit (Catalog # EK1001) with Tanon 5200 system. A specific band was detected for PCNA at approximately 35KD. The expected band size for PCNA is at 29KD.

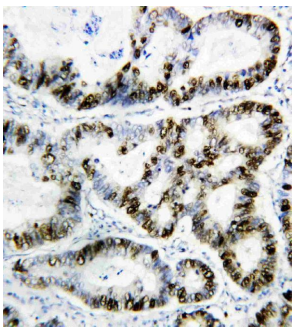

IHC analysis of PCNA using anti-PCNA antibody (MA1083). PCNA was detected in paraffin-embedded section of human Rectal cancer tissues. Heat mediated antigen retrieval was performed in citrate buffer (pH6, epitope retrieval solution) for 20 mins. The tissue section was blocked with 10% goat serum. The tissue section was then incubated with 1ug/ml mouse anti-PCNA Antibody (MA1083) overnight at 4°C. Biotinylated goat anti-mouse IgG was used as secondary antibody and incubated for 30 minutes at 37°C. The tissue section was developed using Strepavidin-Biotin-Complex (SABC)(Catalog # SA1021) with DAB as the chromogen.

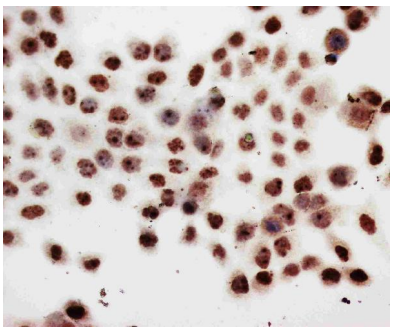

IHC analysis of PCNA using anti-PCNA antibody (MA1083). PCNA was detected in immunocytochemical section of human HELA Cell. Enzyme antigen retrieval was performed using IHC enzyme antigen retrieval reagent (AR0022) for 15 mins. The cells were blocked with 10% goat serum. And then incubated with 1ug/ml mouse anti-PCNA Antibody (MA1083) overnight at 4°C. Biotinylated goat anti-mouse IgG was used as secondary antibody and incubated for 30 minutes at 37°C. The section was developed using Strepavidin-Biotin-Complex (SABC)(Catalog # SA1021) with DAB as the chromogen.

IHC analysis of PCNA using anti-PCNA antibody (MA1083). PCNA was detected in paraffin-embedded section of HepG2 subcutaneous xenograft in nude mice tissues. Heat mediated antigen retrieval was performed in citrate buffer (pH6, epitope retrieval solution) for 20 mins. The tissue section was blocked with 10% goat serum. The tissue

BOSTER BIOLOGICAL TECHNOLOGY
3942 B Valley Ave, Pleasanton, CA 94566
888-466-3604 | support@bosterbio.com | www.bosterbio.com

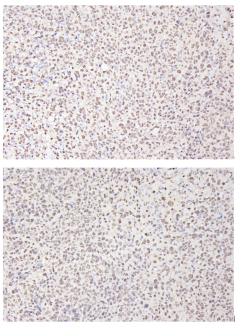

section was then incubated with 1:500 mouse anti-PCNA Antibody (MA1083) overnight at 4°C. Two-step IHC detection kit was used as secondary antibody and incubated for 30 minutes at 37°C. The tissue section was developed using Strepavidin-Biotin-Complex (SABC)(Catalog # SA1021) with DAB as the chromogen.

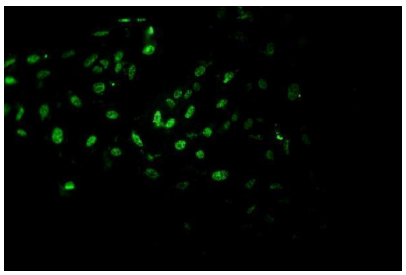

IF analysis of PCNA using anti-PCNA antibody (MA1083). PCNA was detected in an immunocytochemical section of HepG2 cells. Enzyme antigen retrieval was performed using IHC enzyme antigen retrieval reagent (AR0022) for 15 mins. The cells were blocked with 10% goat serum. And then incubated with 1:1000 mouse anti-PCNA Antibody (MA1083) overnight at 4°C. DyLight®488 Conjugated Goat Anti-Rabbit IgG (BA1127) was used as secondary antibody at 1:500 dilution and incubated for 30 minutes at 37°C. The section was counterstained with DAPI. Visualize using a laser confocol.

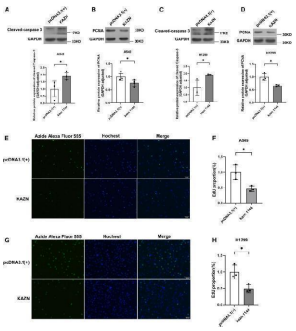

KAZN overexpression inhibits cell proliferation and induces apoptosis. (A and B) Western blot analysis (upper) and quantification (lower) of cleaved-caspase 3 (A) and PCNA (B) levels in A549 cells overexpressing KAZN. (C and D) Western blot analysis (upper) and quantification (lower) of cleaved-caspase 3 (C) and PCNA (D) levels in NCI-H1299 cells overexpressing KAZN. (E and F) EdU staining of A549 cells overexpressing KAZN and quantification of EdU-positive cells. (G and H) EdU staining of NCI-H1299 cells overexpressing KAZN and quantification of EdU-positive cells. Scale bar: 200 um. Data were presented as mean ± SD from at least 3 independent experiments. p values were calculated using the unpaired Student’s t test. ∗p < 0.05.Index in PubMed under a CC BY license. PMID: 41126879

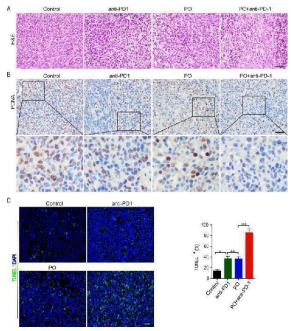

Combination of PO and PD-1 blockade inhibited proliferation and induced apoptosis of tumor in vivo . (A) Paraffin sections of CT26 tumor tissues were analyzed by H&E staining (n = 3). (B) Expression and quantification of PCNA-positive staining in CT26 tumor tissues was examined by IHC using Image-Pro Plus 6.0 and in three random fields (n = 3). Scale bar, 50 um. (C) TUNEL staining and the quantification of TUNEL-positive cells in CT26 tumor tissues (n = 3). Scale bar, 20 um *p < 0.05, **p < 0.01, versus as indicated. ns, not significant.Index in PubMed under a CC BY license. PMID: 39990679

knockdown of RIPK2 suppressed GC cell proliferation and apoptosis in vivo. (A-D) IHC was used to detect the expression of RIPK2 and PCNA in tumor section, and quantification. (E-F) TUNEL was performed to detect the

BOSTER BIOLOGICAL TECHNOLOGY
3942 B Valley Ave, Pleasanton, CA 94566
888-466-3604 | support@bosterbio.com | www.bosterbio.com

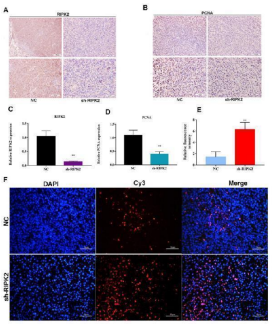

apoptosis cells in tumor section, and the quantification of fluorescent intensity. * P < 0.05, ** P < 0.01.Index in PubMed under a CC BY license. PMID: 38164277

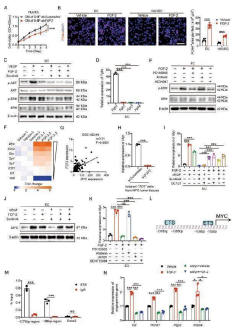

FGF-2 impedes the AAD-induced anti-EC effect via FGFR1-ERK-MYC signaling. A Cell growth of human ECs receiving the conditioned medium of scrambled- or FGF2 shRNA-transfected NPC tumor cells (n = 5 samples per group). B Representative micrographs of PCNA + proliferative cells and DAPI signals in ECs treated with vehicle or recombinant human FGF-2. Scale bar = 50 um. Quantification of PCNA + signals in and human ECs (n = 8 random fields per group). C Vehicle- or VEGF-treated ECs were challenged with or without sunitinib or FGF-2. Phosphorylation of AKT and ERK in ECs was detected. beta-actin marks the loading level in each lane (n = 3 samples per group). D QPCR quantification of Fgfr1 , Fgfr2 , Fgfr3 , and Fgfr4 mRNA levels in ECs (n = 3 samples per group). E Vehicle- or FGF-2-treated ECs were challenged with or without various FGFR inhibitors. Phosphorylation of ERK in ECs was detected. beta-actin marks the loading level in each lane (n = 3 samples per group). F Downstream of VEGF signaling transcription factors were selected and detected in vehicle- or FGF-2-treated ECs. Heatmap of qPCR array screened out Myc as the highest upregulated transcription factor. G Correlation of FGF2 and MYC transcriptomic expression levels of human NPCs (NPC, n = 113 samples). Data was extracted from dataset GSE102349. H QPCR quantification of Myc mRNA levels in isolated CD31 + ECs from scrambled- or FGF2 shRNA-transfected NPC tumor tissues (n = 3 samples per group). I QPCR quantification of Myc mRNA levels in various groups of ECs (n = 3 samples per group). J Vehicle- or VEGF-treated ECs were treated with or without AAD or FGF-2. MYC expression in ECs was detected. beta-actin marks the loading level in each lane (n = 3 samples per group). K QPCR quantification of Myc mRNA levels in vehicle- or FGF-2-treated ECs, with or without various inhibitors (n = 3 samples per group). L Diagram of ETS-binding site prediction. M ChIP detection of ETS binding to the Myc gene promoter. Nonimmune IgG and Myc exon 2 regions served as controls (n = 3 samples per group). N QPCR quantification of EC proliferative marker Kdr , Plxnd1 , Ptgs2 , Robo4 in scrambled- or Myc siRNA-transfected ECs administrated with vehicle or FGF-2 (n = 3 samples per group). * P

Immunohistochemistry staining of wound tissues on days 7 and 14. (A) Representative images for CD31, PCNA, alpha-SMA, and CD68 staining (scale bar = 100 um). (B–E) Quantification of CD31, PCNA, alpha-SMA, and CD68 protein

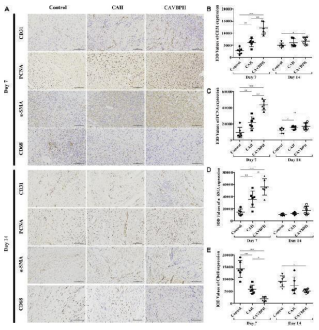

expressions, respectively. * p < 0.05, ** p < 0.01, *** p < 0.001 vs . control group; # p < 0.05, ## p < 0.01, ### p < 0.001 vs . CAH group as statistically significant.Index in PubMed under a CC BY license. PMID: 35784748

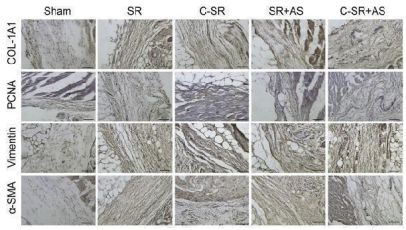

Effect of asiaticoside on the transformation of fibroblasts into myofibroblasts, collagen deposition and fibroblast proliferation in vivo . Immunohistochemical staining of tissue around silicone rubber (SR) and carbon silicone rubber (C-SR) with alpha-SMA, vimentin, PCNA and COL-1A1 (100X).Index in PubMed under a CC BY license. PMID: 35646845

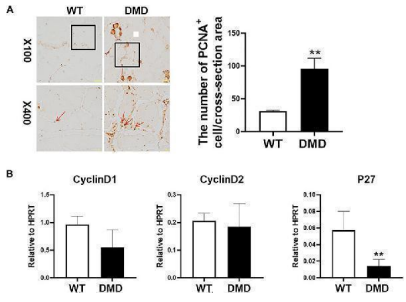

Increase proliferation of muscle cells in tibialis anterior in DMD mice. (A) Immunohistochemical staining of muscle cells was performed with the PCNA antibody. PCNA positive cells are shown as brown (red arrow). The PCNA positive cells were counted under microscope. Numbers of PCNA positive cells were demonstrated in the visual field Data were presented at means ± SEM (n = 6) with independent sample t -test. ** p < 0.01. (B) Gene expression of tibialis anterior cells in WT and DMD mice was detected by RT-PCR. Data are expressed as the mean ± SEM (n = 6). ** p < 0.01.Index in PubMed under a CC BY license. PMID: 35372342

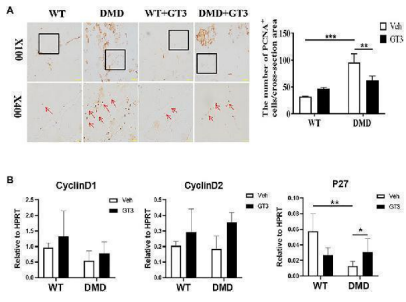

Effects of GT3 on proliferation of muscle cells. (A) The tibialis anterior was extracted 48 h after GT3 treatment in 40-week-old WT and DMD mice. PCNA positive cells were stained with brown (red arrow, left panel). Numbers of PCNA positive cells were counted in each field. Data were presented at means ± SEM (n = 6) with two-way ANOVA analysis. ** p < 0.01, *** p < 0.001. (B) Gene expression of tibialis anterior muscle cells was detected by RT-PCR after GT3 treatment. Data were presented at means ± SEM (n = 6) with two-way ANOVA analysis. * p < 0.05, ** p < 0.01.Index in PubMed under a CC BY license. PMID: 35372342

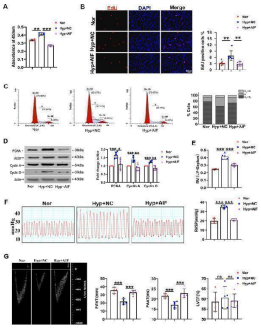

AIF blocks hypoxia-induced progression of PH in vitro and in vivo. A Hypoxia increased the viability of PASMCs after growth arrest for 24 h, and this effect was decreased by AIF (n = 4). B Pretreatment with an AIF overexpression plasmid blocked the effects of hypoxia on EdU incorporation in cells (n = 6). Scale bars: 50 um. C Cell cycle analysis by flow cytometry indicated that hypoxia stimulated cell progression into G 2 /M + S phase, and this effect was inhibited by AIF overexpression (n = 3). D Effects of AIF on the expression of PCNA, Cyclin A and Cyclin D under hypoxia (n = 4–5). E Represents weight ratio of the right ventricular (RV)/left

BOSTER BIOLOGICAL TECHNOLOGY
3942 B Valley Ave, Pleasanton, CA 94566
888-466-3604 | support@bosterbio.com | www.bosterbio.com

ventricular (LV) + Septum (n = 6); F Represents the right ventricular systolic pressure (RVSP) from mice (n = 5); G pulmonary artery velocity time integral (PAVTI), pulmonary artery acceleration time (PAAT) and left ventricular ejection fraction (LVEF) of the hypoxic mouse model infected with AAV5-NC and AAV5-AIF (n = 6). All data are presented as the means ± standard deviation. *p<0.05; **p<0.01; ***p<0.001; Nor normoxia, Hyp hypoxia, NC negative control Index in PubMed under a CC BY license. PMID: 35090552

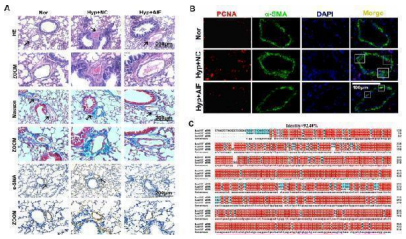

AIF blocks hypoxia-induced pulmonary vascular remodeling in vivo. A Morphological analysis of the pulmonary artery was performed using HE staining and Masson staining, and the thickness of pulmonary vascular medium was measured by alpha-SMA staining (n = 5). B Increased proliferation of the pulmonary vascular cells was visualized by PCNA-positive staining per vascular area under hypoxia compared with exposure to normal conditions at the same time, these effects were reversed by the administration of AAV5-AIF (n = 3). C Homology analysis of the AIF gene among humans, mice and rats. Nor normoxia, Hyp hypoxia, NC negative control Index in PubMed under a CC BY license. PMID: 35090552

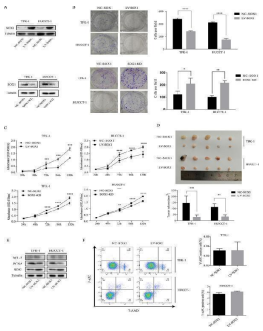

SOX1 inhibits CCA cell proliferation in vitro and suppresses tumor growth in vivo. A TFK-1 and HUCCT-1 cells were transfected with NC-SOX1, LV-SOX1 and SOX1-KD for 72 h. SOX1 protein level was assessed by Western blotting. B Representative images of colony formation assay (left panel) and analysis of colony numbers (right panel). *p

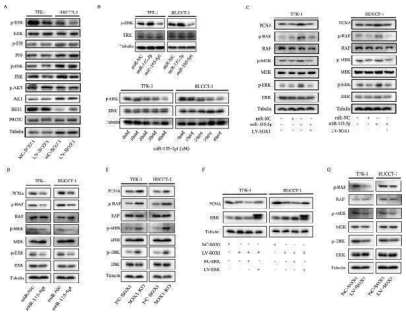

Mir-155-5p inhibits SOX1 leading to activation of the Raf/MEK/ERK pathway. A Cells were transfected with lentiviral negative control vector (NC-SOX1) or lentiviral SOX1 (LV-SOX1) for 72 h. Protein expressions of SOX1, HES1, PROX1, p-AKT, p-JNK, and p-P38 were examined by Western blot. B Above panel: protein levels of ERK and p-ERK in HUCCT-1 and TFK-1 cells transfected with miR-negative control (miR-NC), miR-155-5p-mimic (miR-155-5p), and miR-155-5p-inhibitor (miR-155-5pI). Below panel: TFK-1 and HUCCT-1 cells was treated with different concentrations of miR-155-5pI. The protein level of ERK and p-ERK were detected by Western blot. C Protein levels of central members of MAPK/ERK signaling (RAF, p-RAF, MEK, p-MEK, ERK and p-ERK) and downstream of ERK (PCNA) in TFK-1 and HUCCT-1 cells were detected by Western blot. D TFK-1 and HUCCT-1 cells was transfected with miR-negative control (miR-NC) and miR-15-5p inhibitor (miR-155-5pI), then protein levels of central members of MAPK/ERK signaling (RAF, p-RAF, MEK, p-MEK, ERK and p-ERK) and PCNA were detected by Western blot. E TFK-1 and HUCCT-1 cells was transfected with lenvisual carrying SOX1-RNAi (SOX1-KD),

BOSTER BIOLOGICAL TECHNOLOGY
3942 B Valley Ave, Pleasanton, CA 94566
888-466-3604 | support@bosterbio.com | www.bosterbio.com

then protein levels of central members of MAPK/ERK signaling (RAF, p-RAF, MEK, p-MEK, ERK and p-ERK) and PCNA were detected by Western blot. F Cells were infected with NC-SOX1, LV-SOX1, LV-SOX1 + NC-ERK and LV-SOX1 + LV-ERK, and then detect changes in ERK and PCNA protein levels by western blot. G Protein levels of central members of MAPK/ERK signaling (RAF, p-RAF, MEK, p-MEK, ERK and p-ERK) was detected in xenograft tumor samples which had been transfected with NC-SOX1 and LV-SOX1 Index in PubMed under a CC BY license. PMID: 34876142

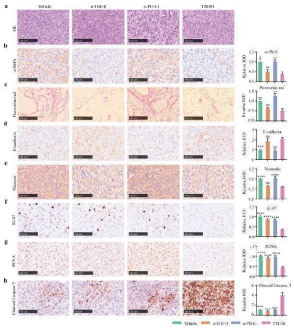

Immunohistochemical staining to evaluate the activity of carcinoma-associated fibroblast, the status of mediated epithelial-mesenchymal transition of cancer cells, as well as the proliferation and apoptosis of cancer cells. a H&E staining. b Anti-alpha-SMA staining. c Picrosirius red staining. d Anti-E-cadherin staining. e Anti-Vimentin staining. f Anti-Ki-67 staining. g Anti-PCNA staining. h Anti-cleaved-Caspase 3. For quantitative analysis, the integral optical density (IOD) of values the IHC stainings were calculated. * p

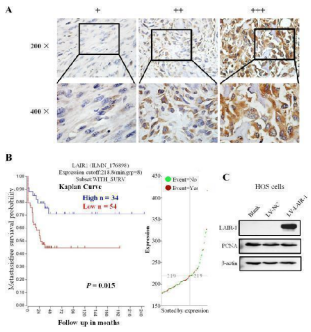

Representative images of different LAIR-1 immunohistochemistry staining intensities in OS tissues. The proportion of positively stained cells for LAIR-1 was calculated by assessing the entire image. Based on the LAIR-1 staining intensities in OS tumor samples, the staining patterns were categorized as follows: weak (+), moderate (++), and intense (+++). Upper panel, original magnification × 200; lower panel, original magnification × 400. b Kaplan–Meier plot of survival rates of patients with tumors exhibiting high (blue line) or low (red line) LAIR-1 expression; data were obtained using the R2 platform. c Western blotting for determining LAIR-1 expression and PCNA proliferation marker levels in HOS cells following LV-NC or LV-LAIR-1 lentivirus infection or without treatment (blank). beta-actin was used as a loading control Index in PubMed under a CC BY license. PMID: 32563267

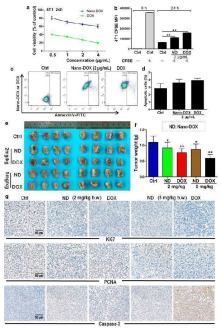

Anti-TNBC efficacy of Nano-DOX in comparison with DOX. a Effects of Nano-DOX and DOX on the viability of 4T1 cells in vitro assayed by the CCK-8 test. b Effects of Nano-DOX and DOX on the proliferation of 4T1 cells in vitro assayed by CFSE staining. c , d Apoptosis of 4T1 cells after 24-h treatment of Nano-DOX or DOX assayed by annexin V immunofluorescent staining and FACS. e , f Size and weight of orthotopic 4T1 tumor xenografts in mice at the end of 3-week treatment of Nano-DOX or DOX. g Immunohistochemical staining of Ki67, PCNA (markers of cancer cell proliferation), and caspase 3 (marker of cancer cell apoptosis) in mouse orthotopic 4T1 tumor xenografts at the end of 3-week treatment of Nano-DOX or DOX. (Duration of Nano-DOX or DOX treatment was 24 h for the in vitro cell experiments.) In FACS analysis, geometric means were used to quantify fluorescence intensity. Values were mean ± SD (n = 3 for in vitro experiments and n = 8 for in vivo experiments, *p<0.05, **p<0.01) Index in PubMed under a

BOSTER BIOLOGICAL TECHNOLOGY
3942 B Valley Ave, Pleasanton, CA 94566
888-466-3604 | support@bosterbio.com | www.bosterbio.com

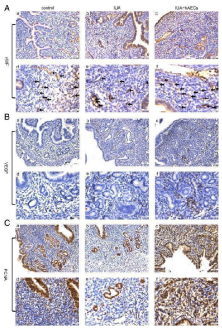

hAECs facilitated endometrial recovery in the IUA mouse model. A IHC staining of vWF reflected the MVD of the endometrium. The microvessels, which were vWF-positive, are indicated by arrows in the figure. MVD was reduced in the IUA group and increased in the hAEC-treated group. B IHC staining showed that the expression of VEGF was higher in the hAEC-treated group than in the IUA group. C The expression of PCNA decreased in the IUA group and reached almost normal levels in the hAEC-treated group. a–c, scale bar = 100 um; d–f, scale bar = 50 um Index in PubMed under a CC BY license. PMID: 31412924

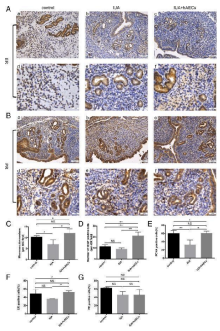

hAECs facilitated endometrial recovery in the IUA mouse model. A According to IHC staining, the number of ER-positive cells was higher in the hAEC-treated group than in the IUA group. B There was no difference in PR expression among these three groups. C VEGF expression was semi-quantified, and the number of positive cells per field was calculated. D MVD was valued by counting microvascular vessels, which were vWF-positive. E – G . PCNA, ER, and PR expression levels were semi-quantified by calculating the percentage of positive cells per field (* p

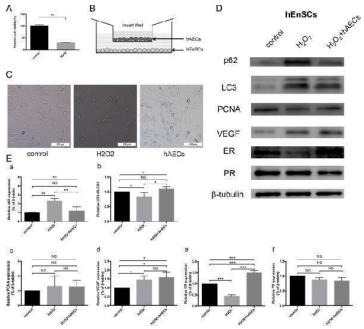

hAECs promoted autophagy in hEnSCs in vitro. A The cell viability of H 2 O 2 -treated hEnSCs significantly decreased. B hEnSCs were cocultured with hAECs in a Transwell system. C After 2.5 h of H 2 O 2 treatment and another 24 h of culture, hEnSCs shrank severely, but hAEC coculture repaired the cell morphology of hEnSCs damaged by H 2 O 2 . D Western blot analysis showed that p62 expression increased significantly in H 2 O 2 -treated hEnSCs and decreased in hEnSCs cocultured with hAECs. The relative expression of LC3-II/LC3-I was decreased in H 2 O 2 -treated hEnSCs and increased in hEnSCs cocultured with hAECs. The expression level of ER was downregulated in H 2 O 2 -treated hEnSCs but upregulated in hEnSCs cocultured with hAECs. The expression of VEGF, PCNA, and PR did not change prominently. E The grayscale values of the western blots were evaluated. The ratios of LC3-II/LC3-I were standardized to those of the control group. The protein levels of p62, PCNA, VEGF, ER, and PR were normalized to that of beta-tubulin (n = 3; * p

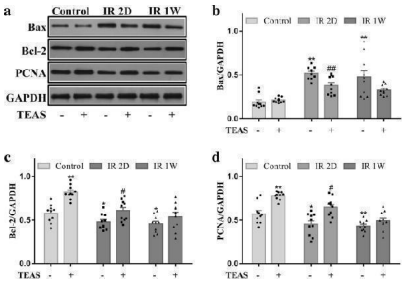

The effect of TEAS on irradiation-induced expression of Bax, Bcl-2 and PCNA proteins in ovary. a The protein expression levels of Bax, Bcl-2, PCNA were determined by western blot analysis. b – d Quantitative analysis of total proteins was represented using a bar graph. The data represent the mean ± SEM. * P

BOSTER BIOLOGICAL TECHNOLOGY
3942 B Valley Ave, Pleasanton, CA 94566
888-466-3604 | support@bosterbio.com | www.bosterbio.com

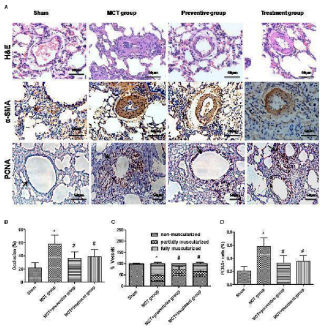

PNU-282987 treatment prevents and reveres pulmonary vascular remodeling. (A) Representative images of hematoxylin and eosin (HE), immunostaining of alpha-smooth muscle actin (alpha-SMA) and proliferating cell nuclear antigen (PCNA) from the lung in the sham, MCT, prevention and treatment groups. HE shows the thickness of the pulmonary artery. Brown staining with alpha-SMA indicates pulmonary artery smooth muscle, whereas brown-stained cells with PCNA represent proliferating pulmonary artery smooth muscle. The arrow indicates PCNA positive cells of the pulmonary artery. Occlusion (%), %vessels and PCNA positive cell (%) were calculated in a millimeter from 10 separate images of different fields. Original magnification: x400. (B) Graph showing the percentage of the median thickness of the arteriole. (C) Graph showing percentage of muscularization after alpha-SMA immunostaining. (D) Graph showing the percentage of PCNA positive cells. The data are summarized as means ± SD. ∗ P < 0.05 versus the sham group and # P < 0.05 versus the MCT group. Results shown are from one experiment (sham group, n = 15; MCT group, n = 8; MCT+protective group, n = 13; MCT+treatment group, n = 11).Index in PubMed under a CC BY license. PMID: 30863307

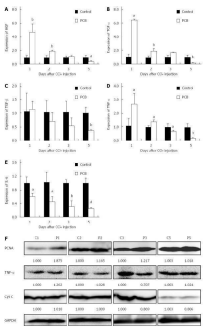

Pathway of phycocyanobilin-accelerated liver regeneration. A-E: Results of real-time quantitative PCR detection at 1, 2, 3 and 5 d after CCl 4 treament. A: The expression of HGF; B: The expression of TGF-alpha; C: The expression of TGF-beta; D: The expression of TNF-alpha; E: The expression of IL-6; F: The western blotting result of PCNA, TNF-alpha, and cytochrome C in liver tissue. C1-C5 indicates the results of the control group from day 1 to day 5, D1-D5 indicates the results of the PCB group from day 1 to day 5. a P < 0.05, b P < 0.01 and d P < 0.001 vs control.Index in PubMed under a CC BY license. PMID: 25987768

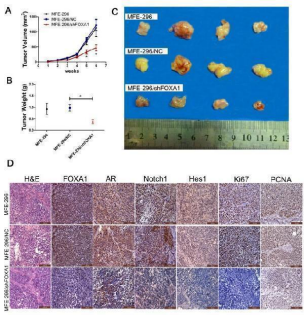

Tumorigenicity assay in nude mice. A : The growth rates of tumors formed from untransfected MFE-296 cells (MFE-296) and MFE-296 cells transfected with NC (MFE-296/NC) or shFOXA1 (MFE-296/shFOXA1). After injection, tumor volumes were calculated every seven days. B and C : Six weeks after injection of MFE-296, MFE-296-NC, and MFE-296-shFOXA1 cells, tumors were removed, and the tumor weights and volumes were determined. Arithmetic means and SD are shown. D : Staining with hematoxylin and eosin (H&E) or immunohistochemical staining for FOXA1, AR, Notch1, Hes1, Ki67, and PCNA in mouse tumor tissues (immunohistochemical staining, 200×). *p<0.05 compared with the NC group. Index in PubMed under a CC BY license. PMID: 24512546

Localization of transplanted cells and in situ proliferation at the infarct border in experimental model . (A-C) are images of coronal cerebral slices showing the impact of occlusion 6 hours post-occlusion, with the infarct appearing as pale area marked with broken line. Hematoxylin and eosin (H.E.) stain illustrates loss of relatively large cells and infiltration of

BOSTER BIOLOGICAL TECHNOLOGY
3942 B Valley Ave, Pleasanton, CA 94566
888-466-3604 | support@bosterbio.com | www.bosterbio.com

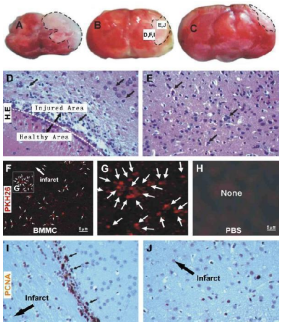

small cells at the border of the infarct (D). Paired cellular profiles are seen peripheral to the infarct border or the infarct penumbra (E). At low magnification, a large number of transplanted bone marrow cells pre-labeled by PKH26 (red fluorescence) are present in the infarct penumbra 7 days post lesion (F). The labeled cells are small and may occur in cluster (G). No fluorescent cells exist in the cerebral cortex of mice received vehicle infusion (H). In situ cell division reflected by immunoreactivity of proliferating cell nuclear antigen (PCNA) occurs predominantly at the infarct border (I) and penumbra (J), appearing as brown immunoreactive nuclei in hematoxylin counter-stained section. Index in PubMed under a CC BY license. PMID: 20973978

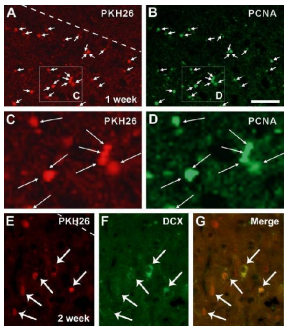

Identification of PKH26-labeled cells with proliferating cell nuclear antigen and doublecortin after transplantation . Colocalization of PKH26-labeled bone marrow cells with proliferating cell nuclear antigen (PCNA) (A-D) and doublecortin (DCX) (E-G) around the infarct penumbra 7 and 14 days following transplantation. PKH26 and PCNA double-labeled cells are small and occur in pair or small cluster (C, D). PKH26 and DCX double-labeled cells have round or oval somata with visible neuronal processes. PKH26 fluorescence appears weaker in these double-labeled cells relative to those seen at 7 days post cell transplantation. Scale bar (in B) = 200 um for A, B and 50 um for C-G. Index in PubMed under a CC BY license. PMID: 20973978

131 Publications Citing This Product

1. PubMed ID: 10.1080/02713683.2019.1657463, The Evaluation of TUNEL, PCNA and SOX2 Expressions in Lens Epithelial Cells of Cataract Patients with Pseudoexfoliation Syndrome

2. PubMed ID: 31562866, Ma Q,Gu JT,Wang B,Feng J,Yang L,Kang XW,Duan P,Sun X,Liu PJ,Wang JC.PlGF signaling and macrophage repolarization contribute to the anti-neoplastic effect of metformin.Eur J Pharmacol.2019 Nov 15;863:172696.doi:10.1016/j.ejphar.2019.172696.Epub 2019 Sep 25.PMID:31562866.

3. PubMed ID: 31505422, Ge Y,Cheng R,Sun S,Zhang S,Li L,Jiang J,Yang C,Xuan X,Chen J.Fangxiao Formula alleviates airway inflammation and remodeling in rats with asthma via suppression of transforming growth factor -beta/Smad3 signaling pathway.Biomed Pharmacother.2019 Nov;119:109429.doi:10.1016/j.biopha.2019.109429.Epub 2019 Sep 7.PMID:31505422.

Visit bosterbio.com/anti-pcna-antibody-monoclonal-ma1083-boster.html to see all 131 publications.

Submit a product review to Biocompare.com

Submit a review of this product to Biocompare.com to receive a $20 Amazon.com giftcard! Your reviews help your fellow scientists make the right decisions. Thank you for your contribution.

Anti-PCNA Antibody (Monoclonal, PC 10)

For Research Use Only. Not for use in diagnostic procedures.